Controls on Water-Column Respiration Rates in a Coastal Plain Estuary: Insights from Long-Term Time-Series Measurements

David Prichett[1,2], Joan Bonilla-Pagan[3], Casey Hodgkins[1], Jeremy M. Testa[1]

[1]Chesapeake Biological Laboratory, University of Maryland Center for Environmental Science, Solomons, MD, USA

[2]Rochester Institute of Technology, Rochester, NY, USA

[3]The Johns Hopkins University, Baltimore, MD, USA

Keywords: Respiration, metabolism, estuary, tides, organic matter, Chesapeake

Abstract

Rates of ecosystem metabolic properties, such as plankton community respiration, can be used as an assessment of the eutrophication state of a waterbody and are the primary biogeochemical rates causing oxygen depletion in coastal waters. However, given the additional labor involved in measuring biogeochemical rate processes, few monitoring programs regularly measure these properties and thus few long-term monitoring records of plankton respiration exist. An eight-year, biweekly plankton community respiration rate time series was analyzed as part of a monitoring program situated in the lower Patuxent River estuary, a tributary of Chesapeake Bay. We found that particulate nutrients (nitrogen and phosphorus) were the most highly correlated co-variates with respiration rate. Additionally, statistical and kinetic models including variables both water temperature and particulate nitrogen were able to explain 74% of the variability in respiration. Over the long-term record, both particulate nutrients and respiration rate were elevated when measured at higher tides. Separate measurements of respiration rate during ten consecutive days and during high and low tide on three separate days also support the enhancement of respiration with high tide. The enhancement was likely due to the import of particulate nutrients from the highly productive mid-bay region. This analysis of the longest consistently measured community respiration rate dataset in Chesapeake Bay has implications for how to interpret long-term records of measurements made at fixed locations in estuaries.

Introduction

Worldwide, the depletion of dissolved oxygen concentrations in estuaries and marine ecosystems is a growing ecological problem. Low dissolved oxygen conditions, often referred to as hypoxia (low oxygen) or anoxia (no oxygen) degrades habitat conditions and can cause mortality or physiological stress for many organisms (e.g., Diaz and Rosenberg 2008; Breitburg et al. 2018). Oxygen depletion can also trigger a cascade of biogeochemical reactions that lead to elevated recycling of nitrogen and phosphorus (e.g., Conley et al. 2009; Testa and Kemp 2012), potentially sustaining hypoxic conditions. Given that future changes in water temperature, freshwater input, nutrient loading, and sea level will likely alter oxygen dynamics through both physical (e.g., solubility, stratification) and biogeochemical (respiration rates) processes, there is a need to better constrain the growing number of projections of oxygen depletion in estuaries worldwide (Irby et al. 2018; Laurent et al. 2018; Ni et al. 2019; Meier et al. 2019).

Respiration is the primary biogeochemical driver of oxygen depletion, and the organic matter fueling water-column respiration is typically derived from surface water productivity (Kemp et al. 2005; Rabalais et al. 2014). Consequently, elevated eutrophication associated with increases in primary production (Boynton et al. 1982) and/or phytoplankton biomass (e.g., Harding and Perry 1997) often leads to coastal hypoxia and anoxia. Although eutrophication is defined as the *rate of input* of organic matter into aquatic ecosystems, it is typically assessed using more easily available concentration or "state" measures (e.g., chlorophyll-a, dissolved oxygen, or nutrient concentrations) because they are less expensive and more readily available than rates of biogeochemical processes (Testa et al. 2022). Thus, a more accurate assessment of eutrophication would involve using measures of biogeochemical rate processes (e.g., respiration) that provide more direct estimates of the relevant processes that consume oxygen. Moreover, microbial respiration has been identified as a critical, yet unconstrained rate process in the ocean despite its relevance for deoxygenation (Robinson 2019).

Despite the value of biogeochemical rate processes for understanding eutrophication and associated oxygen depletion, few long-term, consistently measured rates of these processes have been collected in the coastal zone. For example, in the few systems where measurements of sediment-water fluxes of oxygen and nitrogen (proxies for sediment respiration) have been collected over multiple decades, clear metabolic signals of reduced eutrophication have been identified as nutrient loads have been reduced (Taylor et al. 2020; Testa et al. 2022). Perhaps more numerous are long-term records of plankton primary productivity, given the widespread application of the ^{14}C method since the mid-20th century (e.g., Boynton et al. 1982; Cloern and Jassby 2010) and the growing accuracy of remote-sensing or biogeochemically-derived estimates (Benway et al. 2019). In contrast, few long-term records of water-column community respiration have been collected in estuaries, despite the central roles these rates play in our understanding of oxygen depletion and in constraining models used to predict oxygen depletion into the future. This gap exists despite the fact that many monitoring programs have been collecting estuarine biogeochemical and 'water quality' data for over four decades.

Here we report on an analysis of a 8-year, monitoring effort to measure surface water community respiration rates in a single location at the mouth of the Patuxent River estuary where it exchanges with Chesapeake Bay, in eastern North America. The Patuxent River is a coastal plain tributary of the Chesapeake Bay that experiences depleted oxygen conditions during the summer (Jordan et al. 2003). The goals of this analysis were (1) to develop a suite of statistical and numerical models to determine which factors influenced respiration rate variability, toward a greater understanding of how these rates will be influenced by future change, and (2) make these measurements available to the numerical modeling community better constrain projections of climate effects and management actions. We hypothesized that variability in respiration rate would be elevated by temperature and freshwater inputs through physiological stimulation and the import or production of organic substrate, but we also hypothesized that respiration would also be enhanced through the influence of labile organic matter import from adjacent Chesapeake Bay. This study highlights how long-term hydrographic and biogeochemical measurements can be used to assess controls on the eutrophication state of a tidal estuary and how they would benefit long-term water monitoring programs.

Methods

Study Site and Biogeochemical Data

The Chesapeake Biological Laboratory (CBL) has maintained daily monitoring of temperature and salinity at its research pier since 1938 (Beaven 1960) and has recently (2015) installed a comprehensive environmental monitoring system (https://cblmonitoring.umces.edu/). The CBL pier is situated in the lower Patuxent River estuary where the Patuxent meets the mainstem of Chesapeake Bay (Fig. 1). The water depth at the site is 2.5 m and surface and bottom salinity measurements verify that the water-column is consistently well mixed. We made biweekly measurements of dissolved inorganic nitrogen (ammonium, nitrate + nitrite), orthophosphate, total dissolved phosphorus and nitrogen, total suspended solids, particulate phosphorus, carbon, and nitrogen, and active chlorophyll-a, (Fig. 2 B, C) using standard methods at the Chesapeake Biological Laboratory Nutrient and Analytical Services Laboratory (NASL; https://www.umces.edu/nutrient-analytical-services-laboratory). At each sampling, a YSI Pro 30 was used to measure surface and bottom water temperature and salinity (Fig. 2D). Water-column community respiration rate was also measured biweekly by incubating triplicate 300 mL

borosilicate bottles in-situ, suspended ~1 m below the water surface, and measuring the change in oxygen concentration over the course of the incubation (Fig. 2A). Oxygen was measured within 5 minutes of collection via a YSI ProDO optical oxygen meter (sensor accuracy is reported to be ±0.1 mg/L) and incubations were either 6 hours long (May to October) or 24 hours long (November to April). Bottles were painted black and wrapped in opaque bags before being incubated in-situ from a floating pier in the same location where sample water was collected. Rates were considered to be non-detectable if oxygen did not decrease during the experiment, and we assigned a zero value to these rates. We ran models where these zero values were omitted from the dataset, and the model results were not different. This analysis uses the entire time-series made from March 2015 to December 2022, using the mean of the triplicate respiration rates as the daily value. We also measured respiration rates at higher frequencies during targeted experiments on two occasions, using the same methods as previously described. First, we sampled on 10 consecutive days between June 27th and July 11th, 2016 (Bonilla-Pagan 2016), where community respiration was measured at the same time (~9:30 AM) each day, along with the associated biogeochemical measurements of the pier monitoring program. In this way the tide height and stage changed for each day, but the sampling time stayed constant. Secondly, we measured community respiration and particulate nitrogen (PN) on 3 consecutive days between July 25-27, 2023, but sampled at the time of both high and low tide each day. Tide stage was determined using water level data collected by the National Oceanographic and Atmospheric Administration tide gauging station location on the CBL Pier (NOAA Tides and Currents station 8577330, Solomons Island, Maryland).

Statistical Analysis

The relationship between community respiration rate (hereafter 'respiration rate') and all variables measured in the pier monitoring program was first examined by performing linear regression. We then sought to predict the respiration rate with two types of existing models designed for water quality assessment. First, we applied generalized additive models (GAM) that incorporated terms for season, year (i.e., a long-term trend), and variability in water-column conditions. We used a GAM approach that is comparable to those used for evaluation of ecosystem response to nutrient reduction efforts (Murphy et al. 2019), but here we performed hypothesis testing using different environmental predictors of respiration rate. The GAMs estimate respiration rate from the sum of smooth functions of independent variables. The first model, called the "base" GAM model, only included terms for season and year (Eq. 1):

$$Respiration\ Rate = C + f_1(Year) + f_2(Day\ of\ Year) \quad (1)$$

where the *Day of Year* function was sinusoidal and approximated the annual water temperature cycle. The secondary models included additional terms relative to the base GAM, including functions for temperature, river discharge, chlorophyll-a, dissolved nutrients, and particulate nitrogen (PN) concentration. Model assessment revealed that the base model with a term for PN explained the highest amount of variability in the respiration rate (Eq. 2).

$$Respiration\ Rate = C + f_1(Year) + f_2(Day\ of\ Year) + f_3([PN]^2) \quad (2)$$

The GAM models were generated using the gam() function in the mcgv package in R (Wood 2018). We also modeled respiration rate with a kinetic model comparable to formulations commonly used to estimate phytoplankton respiration in water quality models (Testa et al. 2014; Cerco et al. 2000). This kinetic model estimates respiration rate as a function of temperature and PN concentration (Eq. 3).

$$Respiration\ Rate = k * \theta^{(Temp-20)} * [PN]^2 \quad (3)$$

where k is the respiration rate at 20 ^{o}C, θ is the temperature sensitivity coefficient (1.08), and $Temp$ is water temperature at the time of the rate measurement. We solved for the value of k in the kinetic model by finding the value that generated the smallest sum of squares in the model-observation comparison. To assess the goodness of fit of each model in reproducing the observed respiration rate, three different statistics were computed: sum of squares error (SSE), the correlation coefficient squared (r^2), and the root mean squared error (RMSE). The SSE is the sum of the squared differences between the estimated and observed values where values close to zero indicate less variation measured in the units of the observed values squared. The r^2 statistic measures the tendency of the estimated values and the observed values to vary together, where values vary from 0 to 1 with ideal values close to one (Stow 2009). RMSE is a measure of the size of the differences between estimated and observed values, measured in units of the observed values where values near zero indicate a close match (Stow 2009).

Tidal controls on particulate matter

We then sought to understand what forcing variables at this location influenced PN and thus the respiration rate. GAMs that included Susquehanna River and Patuxent River discharge did not reproduce the observed variability in respiration rate. Prior analysis of a 10-day time-series of respiration at this location suggested a tide-stage effect on respiration (Bonilla-Pagan 2016), and given that this location is at the interface of the Chesapeake Bay and the lower Patuxent estuary, we suspected that high-productivity Chesapeake Bay water could influence this site. Thus, the relationship of the tidal stage versus the respiration rate was examined in more detail. First, we compared respiration rate during ebbing tide to the respiration rate measured during flooding tide. A Student's t test was used to determine if the respiration rates differed by tide stage. The respiration rate and PN concentration data were then separated by tide height into groups of 0.125 m. Kruskal-Wallis rank sum tests was used to determine if the mean respiration rate or mean PN concentration of the tide height groups were different, with a Dunne's post-hoc used for pairwise comparisons.

Results

This analysis of an eight year time series of respiration rate and key associated environmental variables suggests several time scales of variability (Fig. 2). Respiration rate had a regular seasonal cycle, with higher rates during the summer period with higher temperatures, and respiration rate was positively related to water temperature (linear regression, $r^2 = 0.4$, $p < 0.001$). PN, chlorophyll-a, and salinity also had somewhat regular seasonal patterns that were sometimes interrupted by more episodic variability (Fig. 2). For example, PN, salinity, and chlorophyll-a had a consistent seasonal cycle in the first three years of the record (2015-2017) that was interrupted by a large increase in chlorophyll-a and PN in 2018 (and an associated

reduction in salinity and increase in respiration rate), followed by a three year period with less substantial seasonal cycles (Fig. 2). After the 2018 low-salinity event, which was associated with a record precipitation period (see Discussion), chlorophyll-a and PN were somewhat elevated with lower variability and respiration rates reached higher seasonal maxima (Fig. 2).

The particulate nutrient concentrations (nitrogen, phosphorus, and carbon) were the only variables tested aside from temperature that explained substantial variability in respiration rate ($r^2 > 0.25$). Linear regression results indicated that particulate carbon had an r^2 of 0.285, while particulate phosphorus and nitrogen had an r^2 of 0.542 and 0.514 respectively (Fig. 3). Consequently, particulate nutrient concentrations were the only variables whose inclusion in GAMs led to high predictability for respiration rate, where the PN-based GAMs resulted in the best goodness of fit measures (Table 1) relative to other models (note the same model with PP yielded similar results; $r^2 = 0.72$ and RMSE = 0.29). The base GAM model only captured the overall trend and seasonality in the respiration rate, and GAMs with freshwater discharge, water temperature, and chlorophyll-a as predictive terms did not reduce SSE, RMSE, or r^2 (Table 1). Only the PN-based GAM and the kinetic model were able to capture the larger periods of variability in the respiration rate time-series (Fig. 4). Because PN and PP explained more variability in respiration rate than PC, we also built GAMs with the PC:PN and PC:PP ratio with the assumption that these variables, like PN and PP, reflect organic material lability. These models did not perform better than the PN-only models. We also ran the models after removing the zero values from the dataset, and the resulting models only improved the model fits slightly (RMSE = 0.37, 0.35, 0.27 for the Kinetic, Base GAM, and PN-GAM, respectively).

The respiration rates measured at the same time of day during a 10 day period in 2016 were positively, but weakly related with tidal height (Fig. 5; $r^2 = 0.29$; Bonilla-Pagan 2016). The 2023 experiment, which sampled twice a day (at high tide and low tide) during a 3 day period, found that the respiration rate was higher at high tide compared to low tide on two of the three days sampled (Fig. 6). In the two days where respiration rates were higher at high tide, surface water PN concentrations were also higher at high tide (Fig. 6). Given the apparent relationship between tidal height and respiration rate, we examined the relationship of these variables over the long-term respiration rate data set. The difference in the respiration rate during the ebbing tide was not different than the respiration rate during the flooding tide at a significance level of 0.05 ($p = 0.766$). However, there was a difference in the respiration rate at different tide heights at a significance level of 0.05 ($p = 0.00123$). Specifically, the respiration rates at tide heights of 0.25-0.375 m were larger than 0-0.125 m (Fig. 7). As the tide height increased, the upper limit of the respiration rate increased (Fig. 7). The patterns of PN over different ranges of tide height also had a similar relationship as respiration rate (higher PN at higher tide; Fig. 4). However, there was not a difference in the PN at different tide heights at a significance level of 0.05 ($p = 0.3$).

Discussion

This analysis aimed to determine which factors were most important in affecting variability in the respiration rate using a rare long-term record. Global syntheses have found that water column respiration is the dominant sink for oxygen in waters deeper than 10 meters, and even in shallower systems like the one described here, water-column respiration can be 50% of total oxygen consumption (Boynton et al. 2018). Thus, any advance in understanding controls on water column respiration will help improve our understanding of oxygen depletion and thus our

ability to effectively represent this process in models. We found that water temperature and particulate nutrients (carbon, phosphorus, and nitrogen) were most strongly related to respiration compared to all other variables measured, and that models that included both water temperature and particulate nutrients (PN and PP) best reproduced the temporal variability in respiration. Both respiration rates and PN tended to be elevated at high tide, suggesting that the local metabolic rates are sensitive to transport of organic-enriched waters from adjacent habitats.

Water temperature has been well-described as a strong seasonal driver of respiration in Chesapeake Bay (e.g., Smith and Kemp 1995), and this variable was an important factor in predictive models (GAM, kinetic model) of respiration rate developed in this study. This is consistent with a wealth of literature describing the positive relationship between temperature and respiration rate across various ecosystems and methods (Yvon-Durocher et al. 2012; Caffrey et al. 2014; Bordin et al. 2023; Wikner et al. 2023). Although the record of respiration measurements in this study was not long enough to address climate-scale warming trends that have been detected at this location (Orth et al. 2017), the strong temperature effect suggests that future increases in temperature could contribute to higher respiration rates at this location. Water temperature only explained 40% of the variability in the respiration rate in this dataset, however, suggesting that other variables control variability in these rates.

The inclusion of PN or PP in both the GAM and kinetic model increased the power of the models to reproduce variability in the respiration rate. This is consistent with the fact that respiration rate can be amplified with nutrient enrichment (Del Giorgio 2005), whereby elevated nutrient loads lead to elevated uptake of inorganic nutrients and thus incorporation into particulate matter. Estuarine particulate matter is composed of both living and dead organic material, and thus represents both actively respiring phytoplankton and microbially-driven oxidation of detritus. This is consistent with recent global syntheses that found organic material to be as strong a predictor of respiration as temperature (Wikner et al. 2023). The fact that PN was more correlated with respiration than dissolved organic nitrogen (DON) suggests that either the DON pool as measured was not reflective of labile dissolved organic material, or that algal respiration (whereby higher PN = higher algal biomass) is a dominant component of the measured rates. The fact that a squared term for PN provided a better fit in both the GAM and kinetic models reflects the possibility that PN may represent both non-living PON and actively growing algal cells. PN and PP had a much higher correlation with respiration compared to PC, suggesting that labile, newly-produced organic matter is supporting respiration and consistent with the fact that the middle and lower reaches of Chesapeake Bay are less influenced by the bulk carbon pool (Smith and Kemp 1995).

The influence of episodic events and other physical factors on respiration rates were also evident in the variations in respiration rate. Although freshwater discharge and salinity were not substantial contributors to predictive models (Table 1), the effect on respiration of a large precipitation and discharge event is evident in the record (e.g., Fig. 2). In 2018, parts of Maryland, including the Patuxent River watershed, experienced record precipitation levels (NOAA 2019) and during this event the respiration rate was 1.5 to 2 times above the typical summer peaks (Fig. 2A). Both PN and chlorophyll-a peaked during this period, suggesting that elevated riverine flows supported additional algal growth and respiration (Boynton and Kemp 2000; Chen et al. 2009). This sensitivity to large river flow events is consistent with prior

analyses that showed phytoplankton biomass in the Patuxent River estuary to be highly responsive to freshwater discharge (Testa et al. 2008).The fact that discharge and salinity were not good predictors of respiration rate over the entire record, however, is due to the fact that the lower Patuxent is influenced by both the Patuxent River and the Susquehanna River (through exchange with Chesapeake Bay), whose discharge volume and timing are distinct. As a result, high and incoming tides can often have lower salinity than ebb/low tide (data not shown), owing to the fact that the mainstem Bay can have low salinity when Susquehanna River discharge (whose watershed extends >300 km to the north) has been high.

Perhaps the most surprising result of this analysis was the positive correlation of respiration rate with tide heights across the three types of analyses and experiments performed. Because PN was also observed to have a positive relationship with tide height, this effect of tide may simply reflect a higher productivity within adjacent waters that transit the site. Respiration rate was also higher at the lowest PC:PN ratios (Kruskal-Wallis, $p = 0.2$), suggesting that the most N-rich organic material enhances respiration. Given the proximity of the mainstem Chesapeake Bay to this location (Fig. 1) and an assumption that high tide waters are Chesapeake Bay-derived, we hypothesized that the study site is highly influenced by adjacent waters. The fact that high tide associated positively with respiration while there were not differences between flood and ebb rates likely results from the fact that tidal velocities are out of phase with water level at this site and because there are asymmetries in flood and ebb velocities (data not shown). The region of Chesapeake Bay that exchanges with the lower Patuxent estuary is the most productive region of the Bay (Smith and Kemp 1995; Feng et al. 2015), is rich with labile organic matter, and has been previously found to influence productivity in the lower Patuxent estuary (Testa et al. 2008). This result is consistent with other studies that have found an influence of organic material from Chesapeake Bay on metabolic properties in the lower reaches of other Chesapeake Bay tributaries (e.g., Lake and Brush 2008), while import of organic matter from adjacent seaward waters has been implicated in supporting local respiration rates (Smith and Hollibaugh 1997). Despite the evidence presented here to suggest the influence of tide height at the study location, there still remains substantial unexplained variability in the respiration rates, reflecting the varied factors that drive metabolism in estuaries. For example, the suggestive, but inconsistent relationship between tide height and respiration over the consecutive day experiments could result if conditions stimulated organic matter production during prior days and in adjacent water, leading to elevated respiration measured at the site. Future work could address this hypothesis.

The estimates of respiration rate presented here are comparable to in magnitude to similar measurements made in Chesapeake Bay, but differ from a range of other types of estuarine environments. In Chesapeake Bay, Smith and Kemp (1995) measured respiration rates in mainstem surface waters, with rates ranging from 0.2 to 2.0 g O_2 m^{-3} d^{-1} in the mid-Bay region over an annual cycle, where the annual mean (± SD) of rates measured in this study were 1.3 ± 0.3 g O_2 m^{-3} d^{-1}. Smith and Kemp (2003) also measured respiration rates of 1.2 g O_2 m^{-3} d^{-1} in August at 38^{o}N, comparable to the long-term mean of this study's August rates of 1.1 ± 0.2 g O_2 m^{-3} d^{-1}, and reinforcing the potential influence of mainstem waters on the lower Patuxent estuary. These summer rates are also comparable to those measured near the study site in the Patuxent River during June-August 1967, where Flemer and Olmon (1967) reported surface water rates of 0.9 to 1.5 g O_2 m^{-3} d^{-1}. The Patuxent rates were typically higher than many other estuaries and coastal shelves, whose rates were typically less than 1.0 g O_2 m^{-3} d^{-1} and whose mean was

typically less than 0.5 g O_2 m^{-3} d^{-1} (e.g. Dortch et al. 1994; Smith and Hopkinson 2005). This may reflect the fact that the Patuxent River estuary remains a eutrophic estuary, resulting from high rates of nutrient loading (Testa et al. 2008). However, the Patuxent rates were lower than those measured in historically highly eutrophic estuaries (e.g., Roskilde Fjord; Jensen et al. 1990), in some lagoons (Herrera-Silveira 1998) with presumably high residence times, and in shallow nearshore environments (Caffrey et al. 2004) that are often influenced by wetlands and are highly productive.

An analysis of 8 years of regularly measured respiration rates at a fixed station identified multiple controls on metabolic rates in coastal ecosystems. These rates are not typically included in eutrophication assessments because of the higher cost associated with measuring biogeochemical rates (Testa et al. 2022), but this analysis highlights the value of collecting such time-series. These findings are relevant for water quality management in Chesapeake Bay, revealing that some regions of tributary water bodies are highly influenced by adjacent water parcels at tidal time scales. These results also offer a way to test numerical model formulations for a key metabolic rate (respiration or oxygen consumption), possibly improving their ability to make accurate predictions of the effects of climate and nutrient management. We conclude that similar respiration data measured by the simple, fast approach used in this study could be more widely implemented and lead to better assessments of eutrophication.

Acknowledgements

We thank the Chesapeake Biological Laboratory for their support of the Patuxent Sentinel Monitoring Program and to Jerome Frank and the Chesapeake Biological Laboratory Nutrient Analytical Services Laboratory (NASL) for processing water samples for nutrients, chlorophyll, and particulate matter. We would also like to thank current and prior CBL colleagues and members of the Testa Lab for their participation in the Patuxent Sentinel Monitoring Program. This project was partially supported by a Maryland Sea Grant REU program funded by the National Science Foundation. Initial funding for the Pier monitoring system came from a National Science Foundation grant (OCE-1756244) co-authored with Lora Harris and Thomas Miller. We also would like to thank the United States National Oceanographic and Atmospheric Administration (NOAA) for the tide/meteorological data used in this project. Walter Boynton provided helpful feedback on this manuscript. This is UMCES Contribution number XXXX and CBL Ref. No. XXXX-XXX.

References

Beaven, G.F., 1960. Temperature and salinity of surface water at Solomons, Maryland. Chesapeake Science 1: 2-11.

Benway, H.M., Lorenzoni, L., White, A.E., Fiedler, B., Levine, N.M., Nicholson, D.P., DeGrandpre, M.D., Sosik, H.M., Church, M.J., O'Brien, T.D., Leinen, M., Weller, R.A., Karl, D.M., Henson, S.A., and Letelier, R.M. 2019. Ocean time series observations of changing marine ecosystems: An era of integration, synthesis, and societal applications. Frontiers in Marine Sciences 6, 10.3389/fmars.2019.00393.

Bonilla-Pagan, J., Testa, J.M. 2016. Modeling the response to nutrient load reductions in shallow coastal ecosystems. Final Report, Maryland Sea Grant REU Program.

Breitburg, Denise, Levin, L.A., Oschlies, A., Grégoire, M., Chavez, F.P., Conley, D.J., Garçon, V., Gilbert, D., Gutiérrez, D., Isensee, K., Jacinto, G.S., Limburg, K.E., Montes, I., Naqvi, S.W.A., Pitcher, G.C., Rabalais, N.N., Roman, M.R., Rose, K.A., Seibel, B.A., Telszewski, M. Yasuhara, M., and Zhang, J. 2018. Declining oxygen in the global ocean and coastal waters. Science 359.6371: eaam7240.

Bordin, L.H., Machado, E.D.C., Mendes, C.R.B., Fernandes, E.H.L., Camargo, M.G., Kerr, R. and Schettini, C.A. 2023. Daily variability of pelagic metabolism in a subtropical lagoonal estuary. Journal of Marine Systems 240: 103861, https://doi.org/10.1016/j.jmarsys.2023.103861.

Boynton, W.R. and Kemp, W.M., 2000. Influence of river flow and nutrient loads on selected ecosystem processes: A synthesis of Chesapeake Bay data. In: Hobbie, J.H. (ed.) Estuarine science: A synthetic approach to research and practice. Island Press, Washington D.C. 269-298.

Boynton, W.R., Ceballos, M.A.C., Bailey, E.M., Hodgkins, C.L.S., Humphrey, J.L. and Testa, J.M., 2018. Oxygen and nutrient exchanges at the sediment-water interface: A global synthesis and critique of estuarine and coastal data. Estuaries Coasts 41: 301-333.

Caffrey, J.M. 2004. Factors controlling net ecosystem metabolism in U.S. estuaries. Estuaries. 27: 90-101.

Caffrey, J.M., Murrell, M.C., Amacker, K.S., Harper, J.W., Phipps, S. and Woodrey, M.S. 2014. Seasonal and inter-annual patterns in primary production, respiration, and net ecosystem metabolism in three estuaries in the northeast Gulf of Mexico. Estuaries and Coasts 37: 222-241, 10.1007/s12237-013-9701-5.

Cerco, C., Sung-Chan Kim, and M. Noel. 2010. The 2010 Chesapeake Bay Eutrophication Model–A Report to the US Environmental Protection Agency Chesapeake Bay Program and to The US Army Engineer Baltimore District. US Army Engineer Research and Development Center, Vicksburg, MS.

Chen, C.-C., Shiah, F.-K., Chiang, K.-P., Gong, G.-C. and Kemp, W.M., 2009. Effects of the Changjiang (Yangtze) River discharge on planktonic community respiration in the East China Sea. Journal of Geophysical Research: Oceans 114, doi:10.1029/2008JC004891.

Del Giorgio, P., and P.J. le B. Williams (eds.). 2005. Respiration in aquatic ecosystems. Oxford University Press, Oxford, UK.

Díaz, R.J. and Rosenberg, R. 2008. Spreading dead zones and consequences for marine ecosystems. Science 321: 926-929.

Dortch, Q., Rabalais, N.N., Turner, R.E. and Rowe, G.T. 1994. Respiration rates and hypoxia on the Louisiana shelf. Estuaries 17: 862-872.

Feng, Y., Friedrichs, M.A.M., Wilkin, J., Tian, H., Yang, Q., Hofmann, E.E., Wiggert, J.D., and Hood, R.R. 2015. Chesapeake Bay nitrogen fluxes derived from a land-estuarine ocean biogeochemical modeling system: Model description, evaluation, and nitrogen budgets. Journal of Geophysical Research: Biogeosciences 120: 1666-1695, 10.1002/2015jg002931.

Flemer, D.A. and Olmon, J. 1971. Daylight incubator estimates of primary production in the mouth of the Patuxent River, Maryland. Chesapeake Science 12: 105-110.

Irby, I.D., Friedrichs, M.A.M., Da, F. and Hinson, K.E. 2018. The competing impacts of climate change and nutrient reductions on dissolved oxygen in Chesapeake Bay. Biogeosciences 15: 2649-2668, 10.5194/bg-15-2649-2018.

Jensen, L.M., Sand-Jensen, K., Marcher, S. and Hansen, M. 1990. Plankton community respiration along a nutrient gradient in a shallow Danish estuary. Marine Ecology Progress Series 61: 75-85.

Jordan, T. E., Weller, D. E., and Correll, D. L. 2003. Sources of nutrient inputs to the Patuxent River estuary. Estuaries 26: 226-243.

Herrera-Silveira, J.A. 1998. Nutrient-phytoplankton production relationships in a groundwater-influenced tropical coastal lagoon. Aquatic Ecosystem Health and Management 1: 373-385. https://doi.org/10.1016/S1463-4988(98)00015-3.

Hopkinson, C.S. and Smith, E.M. 2005. Estuarine respiration: an overview of benthic, pelagic, and whole system respiration. In: Estuarine Respiration, P. del Giorgio and P.J. le B. Williams (eds). *Respiration in Aquatic Ecosystems*, Oxford University Press, Oxford, UK, 122-146.

Kemp, W.M., W.R. Boynton, J.E. Adolf, D.F. Boesch, W.C. Boicourt, G. Brush, J.C. Cornwell, T.R. Fisher, P.M. Glibert, J.D. Hagy, L.W. Harding, E.D. Houde, D.G. Kimmel, W.D. Miller R.I.E. Newell, M.R. Roman, E.M. Smith, and J.C. Stevenson. 2005. Eutrophication of Chesapeake Bay: Historical trends and ecological interactions. Marine Ecology Progress Series 303: 1-29.

Kemp, W.M., and J.M. Testa. 2011. Metabolic balance between ecosystem production and consumption. Treatise on Estuarine and Coastal Science. Volume 7: 83-118.

Lake, S.J. and Brush, M.J. 2015. Modeling estuarine response to load reductions in a warmer climate: The York River Estuary, Virginia, USA. Marine Ecology Progress Series 538: 81-98.

Laurent, A., Fennel, K., Ko, D.S. and Lehrter, J. 2018. Climate change projected to exacerbate impacts of coastal eutrophication in the northern Gulf of Mexico. Journal of Geophysical Research: Oceans 123: 3408-3426. 10.1002/2017jc013583.

Meier, H.E.M., Eilola, K., Almroth-Rosell, E., Schimanke, S., Kniebusch, M., Höglund, A., Höglund, A., Pemberton, P., Liu, Y., and Väli, G. 2019. Disentangling the impact of nutrient load and climate changes on Baltic Sea hypoxia and eutrophication since 1850. Climate Dynamics 53: 1145–1166.

Murphy, R.R., E. Perry, J. Harcum, and J.L. Keisman. 2019. A generalized additive model approach to evaluating water quality: Chesapeake Bay case study. Environmental Modelling & Software 118: 1-13.

Ni, W., Li, M., Ross, A.C. and Najjar, R.G. 2019. Large projected decline in dissolved oxygen in a eutrophic estuary due to climate change. Journal of Geophysical Research: Oceans. 124: 8271-8289, 10.1029/2019jc015274.

Nixon, S.W. 1995. Coastal marine eutrophication: a definition, social causes, and future concerns. Ophelia 41: 199-219.

Orth, R.J., Dennison, W.C., Lefcheck, J.S., Gurbisz, C., Hannam, M., Keisman, J., Landry, J.B., Moore, K.A., Murphy, R.R., Patrick, C.J., Testa, J.M., Weller, D.E., and Wilcox, D.J. 2017. Submersed aquatic vegetation in Chesapeake Bay: sentinel species in a changing world. Bioscience, https://doi.org/10.1093/biosci/bix058.

Rabalais, N.N., Cai, W.-J., Carstensen, J., Conley, D.J., Fry, B., Hu, X., et al. 2014. Eutrophication-driven deoxygenation in the coastal ocean. Oceanography. 27: 172-183.

Robinson, C. 2019. Microbial respiration, the engine of ocean deoxygenation. Frontiers in Marine Science 5, 10.3389/fmars.2018.00533.

Smith, S.V. and Hollibaugh, J.T. 1997. Annual cycle and interannual variability of net ecosystem metabolism in a temperate climate embayment. Ecological Monographs 67: 509-533.

Smith, E.M. and Kemp, W.M. 1995. Seasonal and regional variations in plankton community production and respiration for Chesapeake Bay. Marine Ecology Progress Series 116: 217-231.

Stow, C.A., J. Jolliff , D.J. McGillicuddy, S.C. Doney, J.I. Allen, M.A.M. Friedrichs, K.A. Rose, and P. Wallhead. 2009. Skill assessment for coupled biological/physical models of marine systems. Journal of Marine Systems 76: 4-15.

Taylor, D.I., Oviatt, C.A., Giblin, A.E., Tucker, J., Diaz, R.J. and Keay, K., 2020. Wastewater input reductions reverse historic hypereutrophication of Boston Harbor, USA. Ambio 49: 187-196, 10.1007/s13280-019-01174-1.

Testa, J.M., Boynton, W.R., Hodgkins, C.L.S., Moore, A.L., Bailey, E.M., and Rambo, J. 2022. Biogeochemical states, rates, and exchanges exhibit linear responses to large nutrient load reductions in a shallow, eutrophic urban estuary. Limnology and Oceanography 67: 739-752.

Testa, J.M., Y. Li, Y.J. Lee, M. Li, D.C. Brady, D.M. Di Toro, and W.M. Kemp 2014. Quantifying the effects of nutrient loading on dissolved O_2 cycling and hypoxia in Chesapeake Bay using a coupled hydrodynamic–biogeochemical model. Journal of Marine Systems 139: 139-158.

Testa, J.M., Kemp, W.M., Boynton, W.R. and Hagy, J.D. 2008. Long-term changes in water quality and productivity in the Patuxent River estuary: 1985 to 2003. Estuaries Coasts 31: 1021-1037.

Wikner, J., Vikström, K. and Verma, A. 2023. Regulation of marine plankton respiration: A test of models. Frontiers in Marines Science 10, 10.3389/fmars.2023.1134699.

Wood, S. 2018. Mgcv, vol. 1. pp. 8–23. https://CRAN.R-project.org/package=mgcv.

Yvon-Durocher, G., Caffrey, J.M., Cescatti, A., Dossena, M., del Giorgio, P., Gasol, J.M., Montoya, J.M., Pumpanen, J., Staehr, and P.A.Trimmer, M. 2012. Reconciling the temperature dependence of respiration across timescales and ecosystem types. Nature 487: 472–476.

Table 1. Goodness of fit statistics for statistical and mechanistic models used to predict respiration rate, including those included in Figure 4 and other experimental models. "with time" represents those models with *Year* and *Day of Year* as model terms.

Model Type	SSE	r^2	RMSE
GAM with time and PN	*14.64*	*0.741*	*0.282*
GAM with time and C:N Ratio	*14.56*	*0.742*	*0.281*
GAM with time and chlorophyll-a	*18.23*	*0.678*	*0.315*
Kinetic Model	*20.49*	*0.669*	*0.334*
GAM with time and temperature	*20.48*	*0.637*	*0.334*
GAM with time and C:P Ratio	*22.78*	*0.597*	*0.352*
Base GAM with time	*22.92*	*0.594*	*0.353*
GAM with time and discharge	*22.90*	*0.593*	*0.353*
GAM with time and salinity	*22.89*	*0.595*	*0.352*

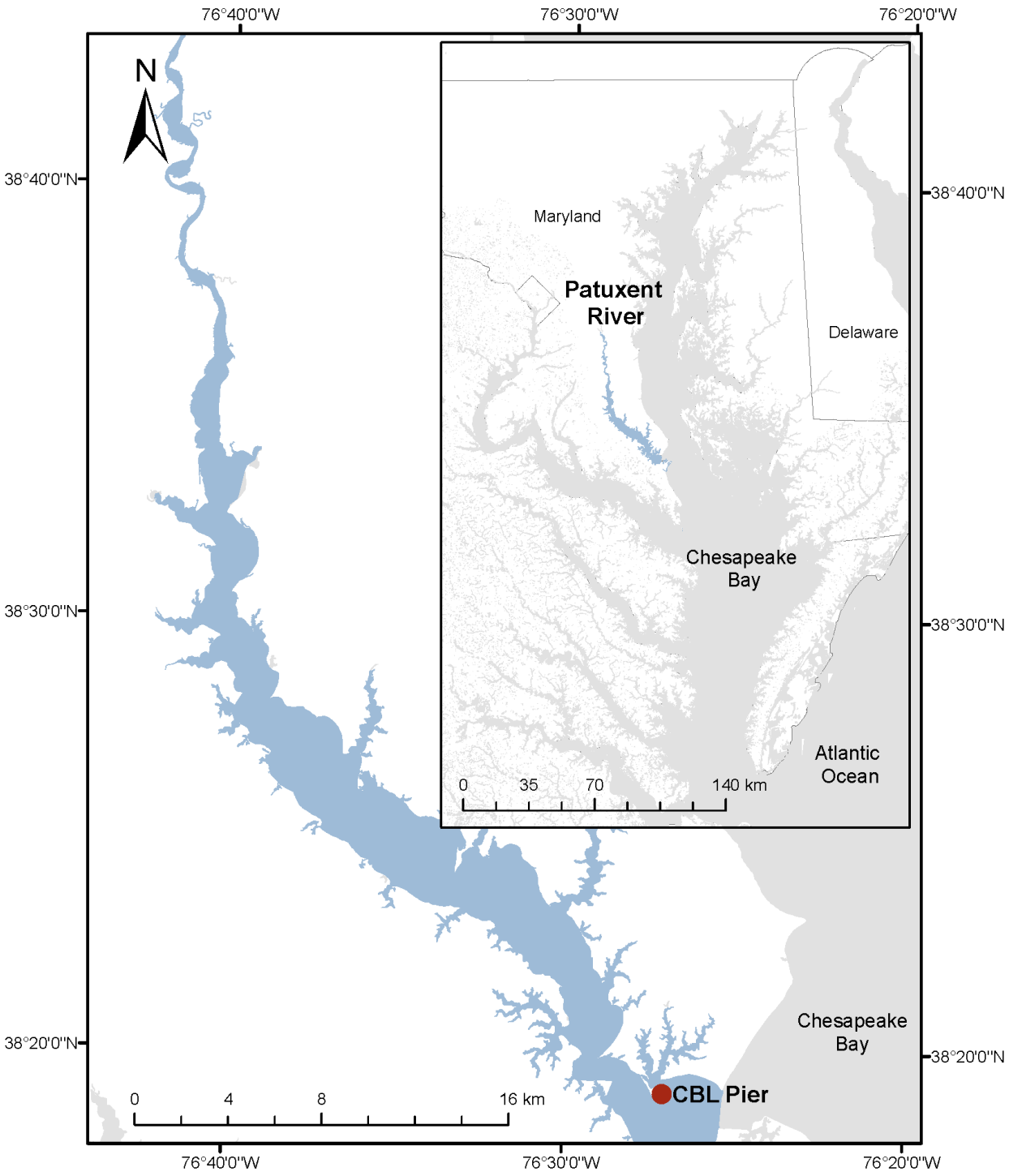

Figure 1: Map of the Patuxent River estuary, including the location of the CBL Research Pier where respiration rates and biogeochemical data were collected. Note location of the Patuxent River on the western shore of Chesapeake Bay in the mid-Atlantic region of the USA.

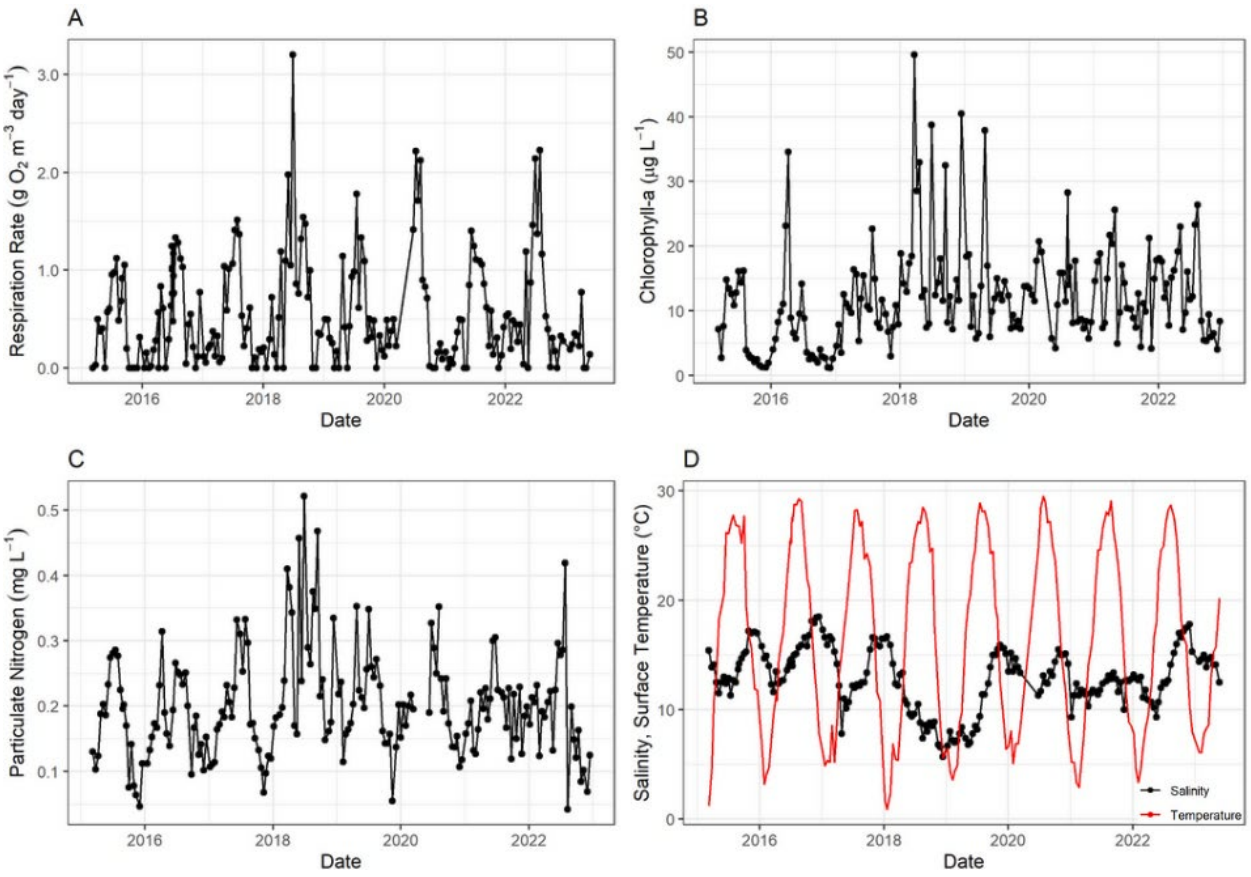

Figure 2. Biweekly measurements of community respiration rate (A), chlorophyll-a (B), particulate nitrogen (C), and salinity (black line) and water temperature (red line) (D) collected from surface water at the CBL research pier monitoring program from 2015-2022.

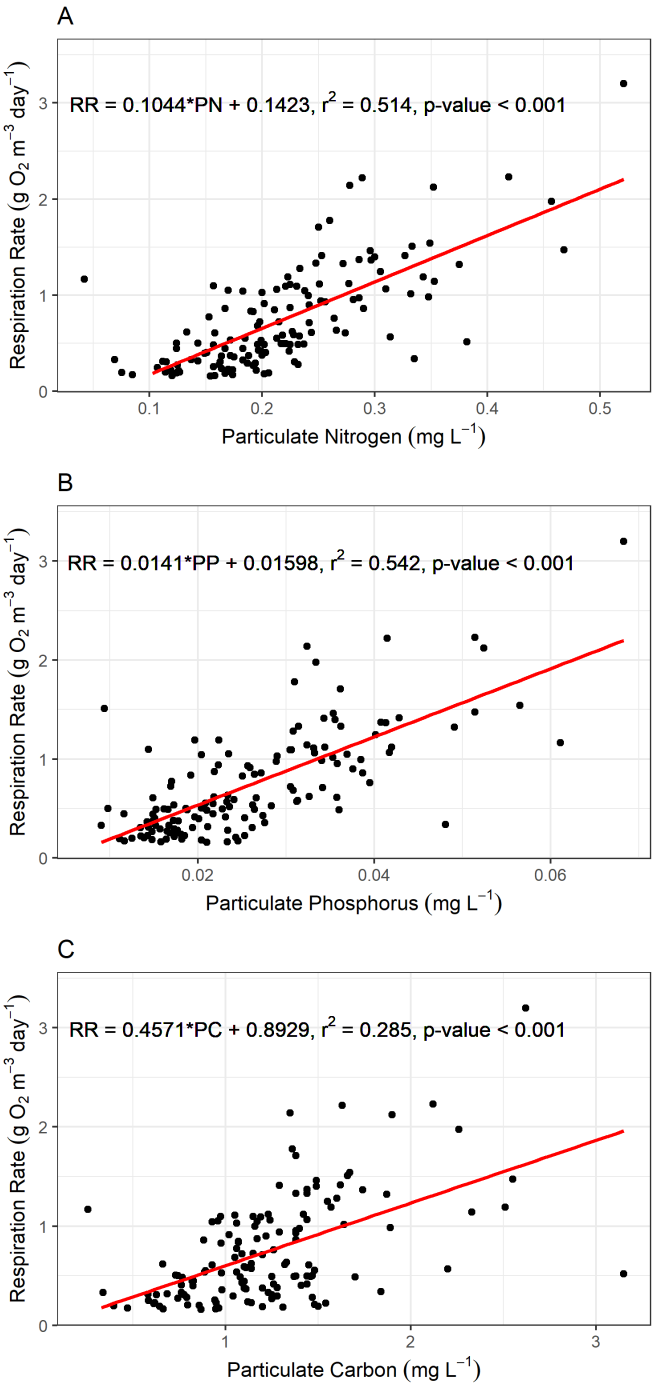

Figure 3. Plots of community respiration rate versus surface water particulate nitrogen (A), particulate phosphorus (B), and particulate carbon (C). Equations for linear regression of respiration rate and particulate material included with corresponding statistics.

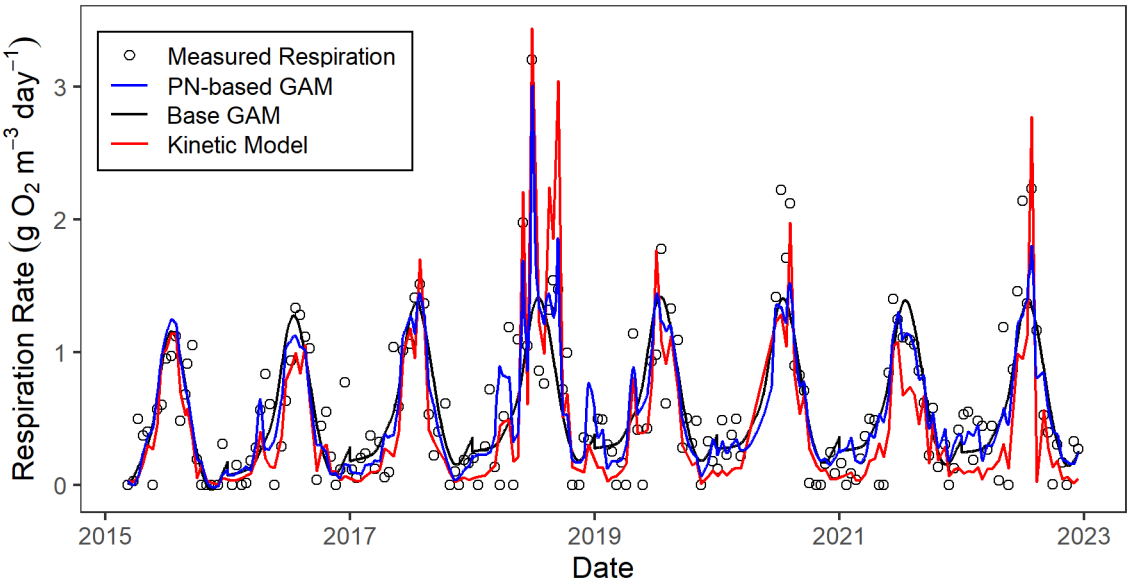

Figure 4. Time-series (2015-2022) of the observed respiration rates (open circles) and the three candidate models, including the time-only GAM (black line), the time- and PN-based GAM (blue line), and the kinetic model (red line).

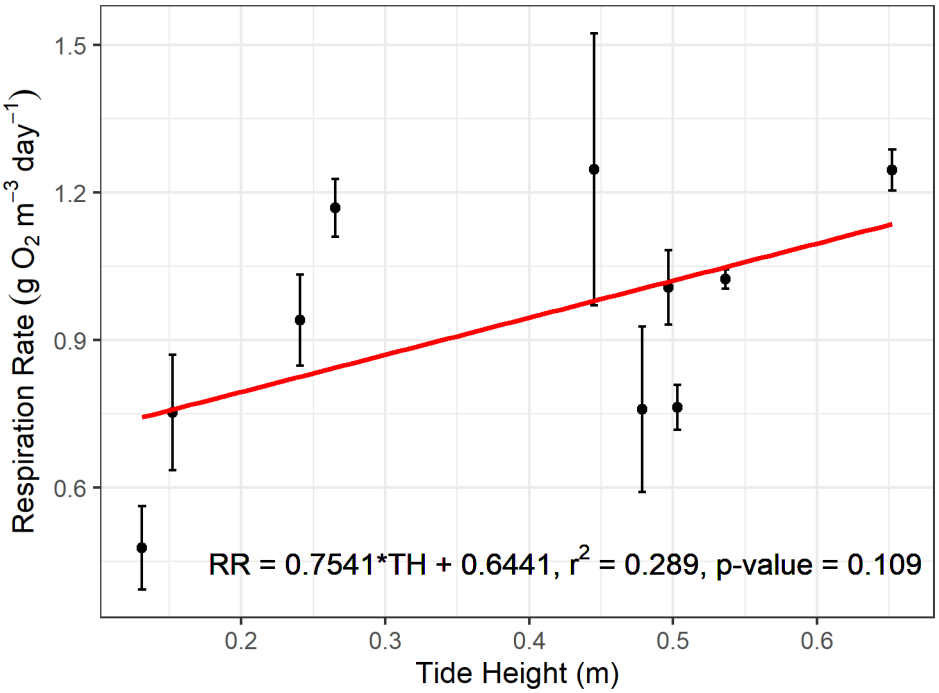

Figure 5. Relationship between respiration rate and mean tide height from the 10-day consecutive sampling carried out in June and July of 2016. Error bars represent the standard deviation of triplicate incubations on each sampling day. Equations for linear regression of respiration rate and particulate material ide height included with corresponding statistics.

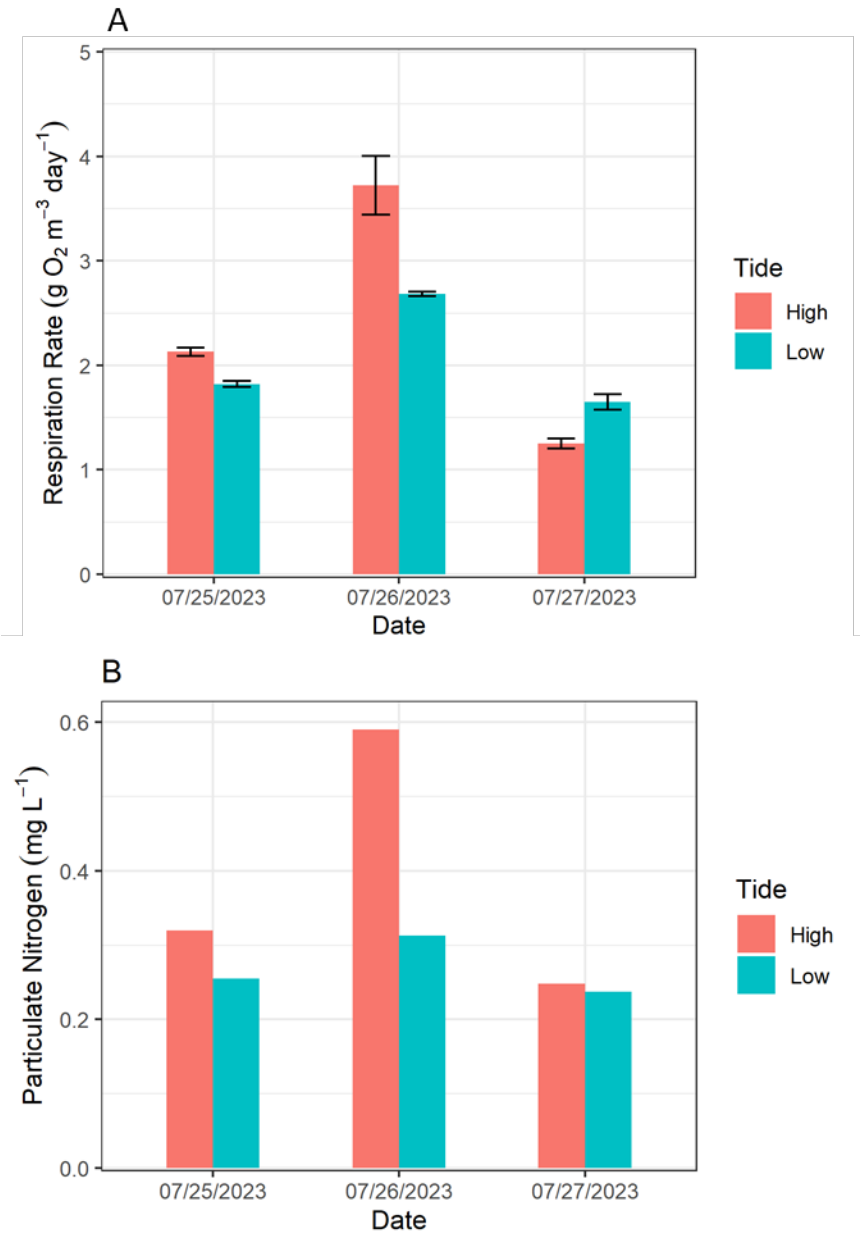

Figure 6. Respiration rate measured at high and low tides from the consecutive 3-day sampling (A, bar = mean +/-SD of triplicate incubations) and particulate nitrogen measured at high and low tides (B, no replicates).

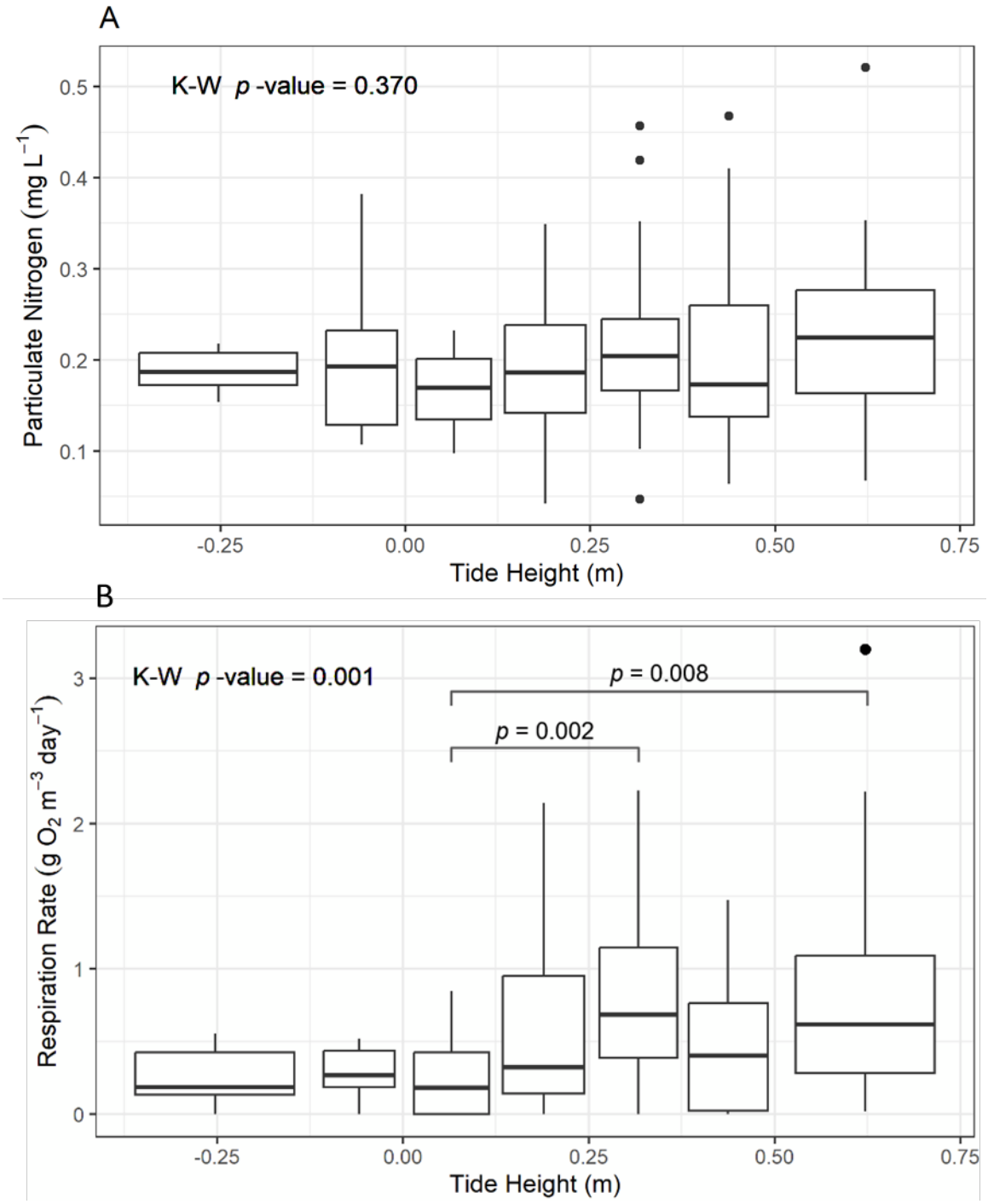

Figure 7. Box plots of surface-water particulate nitrogen (A) and respiration rate (B) aggregated versus ranges of tide height for the bi-weekly samples collected in this study. For each box, the central line is the median, the top and bottom of the box are the 75th and 25th percentiles, respectively, the vertical lines capture the remaining range of the data, and the black circles are outliers. Box widths indicate range of tide heights in group. In panel B, the hatched lines indicate groups whose differences had a p-value less than 0.05 as determined by a Kruskal-Wallis with Dunn's post-hoc comparison.